NJC

Accepted Manuscript

This is an *Accepted Manuscript*, which has been through the Royal Society of Chemistry peer review process and has been accepted for publication.

Accepted Manuscripts are published online shortly after acceptance, before technical editing, formatting and proof reading. Using this free service, authors can make their results available to the community, in citable form, before we publish the edited article. We will replace this *Accepted Manuscript* with the edited and formatted *Advance Article* as soon as it is available.

You can find more information about *Accepted Manuscripts* in the Information for Authors.

Please note that technical editing may introduce minor changes to the text and/or graphics, which may alter content. The journal's standard Terms & Conditions and the Ethical guidelines still apply. In no event shall the Royal Society of Chemistry be held responsible for any errors or omissions in this *Accepted Manuscript* or any consequences arising from the use of any information it contains.

ROYAL SOCIETY OF CHEMISTRY

www.rsc.org/njc

Journal Name

ARTICLE

D-penicillamine and bovine serum albumin co-stabilized copper nanoclusters with remarkably enhanced fluorescence intensity and photostability for ultrasensitive detection of Ag^+

Received 00th January 20xx,
Accepted 00th January 20xx

DOI: 10.1039/x0xx00000x

www.rsc.org/

Li Ruiyi,[a] Wang Huiying,[a] Zhou Xiaoyan,[a] Liao Xiaoqing,[a] Sun Xiulan[b] and Li Zaijun*[,a,c]

Copper nanoclusters (CuNCs) have become promising nanomaterials due to their excellent electronic conductivity and biocompatibility. In the study, we reported a facile synthesis of D-penicillamine and bovine serum albumin co-stabilized copper nanoclusters (BSA/DPA-CuNCs) and the use as optical probe for the detection of Ag^+. Herein, Cu^{2+} was reduced into Cu^0 by D-penicillamine, further leading to form the DPA-CuNCs. Then, the amounts of BSA was introduced into the DPA-CuNCs to obtain the BSA/DPA-CuNCs by their electrostatic attraction. The as-prepared BSA/DPA-CuNCs exhibit remarkably enhanced fluorescence intensity and photostability. The peak fluorescence intensity is more than 2-fold that of DPA-CuNCs. Owing to the synergistic effect between DPA and BSA, the nanosensor based on the BSA/DPA-CuNCs gives ultrasensitive fluorescence response towards Ag^+. Its peak fluorescence intensity linearly decreases with the increase of Ag^+ concentration in the range of 1.0×10^{-8} to 1.0×10^{-16} M with the detection limit of 4.3×10^{-17} M (S/N=3). The method provides the advantage of sensitivity, repeatability and stability, It has been successfully applied in the detection of Ag^+ in water samples. The study also opens a new avenue for the fabrication of functional metal nanoclusters that hold great promise in potential applications such as nanosensors, biocatalyst and molecular carriers.

1 Introduction

Metal nanoclusters (NCs) have attracted great deal of research interest due to their unique physical, electrical and optical properties.[1] Emerging as a new type of fluorescent nanomaterials, the fantastic characteristic of metal NCs has attracted extensive attention, including satisfactory water-solubility, biocompatibility, high quantum yield, good stability and outstanding catalytic property.[2] At present, metal NCs are considered as novel candidate for biosensing,[3] drug controlled release[4] and catalysis.[5] Great effort is paid to the synthesis and application of metal NCs in the recent years.[6] On the account of excellent electronic conductivity and biocompatibility, the development of water-soluble CuNCs produces an extensive importance, especially utilized as essential component in the future nanodevices.[7] However, the synthesis of CuNCs is more difficult compared with other noble metal NCs because CuNC is fairly unstable in the aqueous solution. When it is exposed to air, the surface oxidation will shortly occur. To date, it is still a challenging task to prepare stable CuNCs with bright luminescent, controllable size and shape.[8]

The stabilizer plays key roles in the synthesis of metal NCs. It not only determines the water-solubility of metal NCs and stability in air and water in a certain extent, but also seriously affects on the optical properties, including the fluorescence intensity and photo-stability. Mostly, the stabilizer is also used as the reducing agent and molecular template, thus leading to different reaction rate and particle size and morphology of the final product.[9] Thus, choosing an appropriate stabilizer is the most important work for the specific synthesis. At present, two kinds of stabilizers are widely used for the synthesis of metal NCs. One kind of stabilizers is biomacromolecule such as bovine serum albumin (BSA),[10] transferrin,[11] lysozyme,[12] peptides[13] and DNA.[14] The biomacromolecule often contains a rich of hydrophilic groups and is easy to form an inert shell on the surface of metal cores during the synthesis, which can effectively block the direct contact between the metal core and the oxygen in air. The characteristics make the biomacromolecule-stabilized metal NCs manifest as excellent stability and water-solubility.[15] However, biomacromolecule-stabilized metal NCs often lack of rich functional groups. This greatly limits its applications in the requirement of the specific groups for the specific interaction or chemical reaction. Another kind of stabilizers is small molecule functional reagent such as amino acid.[16] Due to the existence of peculiar functional groups, small molecule-stabilized metal NCs can offer the special interaction or chemical reaction in its application, which further expands their application fields. However, small molecule functional reagent is difficult to form a perfect protective layer on the surface of metal cores, leading to partial exposure of metal cores to air. Small molecule-stabilized metal NCs exhibit a relatively poor stability and water-solubility. By giving full play to their respective advantages, it is possible to create more ideal metal NCs via a perfect combination of above two kinds of stabilizers. As I know, no report is referred to such an ideal.

The study focuses on the synthesis of D-penicillamine and bovine serum albumin co-stabilized copper nanoclusters (BSA/DPA-CuNCs). The as-prepared CuNCs exhibit a higher fluorescence intensity and photostability compared with DPA-CuNCs. The nanosensor based on the BSA/DPA-CuNCs gives ultrasensitive fluorescence response towards Ag^+ owing to synergistic effect between DPA and BSA. The analytical method provides the advantage of sensitivity, repeatability and stability.

2 Experimental

2.1 Materials

D-penicillamine (DPA), bovine serum albumin (BSA), copper nitrate ($Cu(NO_3)_2$) and sodium hydroxide (NaOH) were purchased from Sigma-Aldrich (Mainland, China). Britton-Robinson buffer solution (BR buffer, H_3PO_4-HAc-H_3BO_3, 0.04 M) was prepared and its pH value was adjusted using 0.2 M NaOH solution in the laboratory. Other reagents were of analytical regent grade and were purchased from Shanghai Chemical Company (Shanghai, China). Ultrapure water (18.2 MΩ cm) purified from the Milli-Q purification system was used throughout the experiment.

2.2 Apparatus

Transmission electron microscope (TEM) image was conducted on a JEOL 2010 FEG microscope at 200 keV. The sample was prepared by dispensing a small amount of dry powder in the PBS. Then, one drop of the suspension was dropped on 300 mesh copper TEM grids covered with thin amorphous carbon films. Infrared spectrum (IR) was recorded on a Nicolet FT-IR 6700 spectrometer. X-ray photoelectron spectroscopy (XPS) measurements were performed by using a PHI 5700 ESCA spectrometer with monochromated Al KR radiation (*hv*=1486.6 eV). The pH was measured on the PHS-3D pH meter (Shanghai Precision Scientific Instruments Co., Ltd., China). Fluorescence spectrum and intensity were recorded on a Cary Esclipse fluorescence spectrophotometer (Agilent, Japan). Circular dichroism (CD) measurements were performed on a MOS-450 circular dichroism spectrometer using a 0.01 cm quartz cell. The zeta potential measurement was carried out in ZETASIZER2000 Zeta Potential Analyzer. The absorbance and absorption spectrum were recorded on a TU-1901 spectrophotometer.

2.3 Synthesis of CuNCs

In a typical synthesis, 24 mg of DPA was dissolved in 16 ml of ultrapure water, dropwise added 1.0 ml of 4 mg ml^{-1} $Cu(NO_3)_2$ into the above solution under vigorous agitation. After stirred for 90 min, the solution was filtered with 0.22 nm filter membrane to remove the larger product and by-products. Further, the fluorescent DPA-CuNCs were collected by dialysis against deionized water through a dialysis membrane for 24 h. After that, 0.3 ml of 1mg ml^{-1} BSA solution was added into the DPA-CuNCs under agitation. The solution was continued to stir for 10 min and followed by centrifugation at 4000 r/min for 10 min to remove the larger product. The collected DPA-CuNCs was stored in refrigerator at 4°C for until use.

2.4 Quantum yield measurement

Quantum yield measurement was carried out by dissolving quinine sulphate in o.1 M H_2SO_4 (used as reference). The CuNCs dispersion was used as such. The absorbance of respective sample was measured in the spectrophotometer. Quantum yield was calculated from following equation (1):[17]

$$Q = Q_R \frac{m_s}{m_r} \frac{n_s^2}{n_r^2} \qquad (1)$$

where, Q is the quantum yield of CuNCs, Q_R is the quantum yield of quinine sulphate, m_s is slope of the plot integrated fluorescence intensity *vs* absorbance of CuNCs, m_r is the slope of the plot of integrated fluorescence intensity *vs* absorbance of reference quinine sulphate, n_s and n_r are the refractive indices of the sample and reference, respectively, in the distilled water, which are assumed to be equal to that of water (1.33). The emission spectra for the sample were recorded at excitation wavelength of 320 nm, keeping slit width at 2 nm.

2.5 Synchronous fluorescence spectroscopy

For this measurement, the difference between excitation and emission wavelength (□□Δλ) was set at 15 nm (for tyrosine residues), or at 60 nm (for tryptophan residues). Excitation and emission slit width was set at 2.5 nm.

2.6 Resonance light scattering (RLS) measurement

In the case of RLS analysis, excitation and emission wave-lengths were scanned simultaneously in the wavelength range of 200-800 nm with Δλ=0.

2.7 The procedure for fluorescent detection of silver ion

The BSA/DPA-CuNCs solution (0.6 ml) was mixed with the BR buffer (pH 4.35, 0.4 ml). Then, the Ag^+ standard solution with a known concentration or real water sample (0.6 ml) was added to the above solution. After 30 min incubation, it was subjected to fluorescence measurement on a Cary Esclipse fluorescence spectrophotometer with excitation wavelength of 320 nm. For every Ag^+ concentration, the fluorescence measurement was repeated thrice, and average fluorescence signal was obtained.

3 Results and discussion

3.1 Synthesis of BSA/DPA-CuNCs

In the work, the role of BSA is mainly designed to improve the stability of DPA-CuNC but remain its nanostructure and optical characteristics. The experiment reveals that choosing an appropriate adding order of BSA is essential to achieve the above aim. Firstly, we attempted to add the mixture of DPA and BSA into the Cu^{2+} aqueous solution to prepare BSA/DPA-CuNCs. The resulting CuNCs display a fluorescence spectrum with two emission peaks at 420 nm, corresponding to the BSA-CuNCs, and 642 nm, corresponding to the DPA-CuNCs (shown in Fig.s1). The fact verfies that the use of above method will

result in forming BSA-CuNCs and DPA-CuNCs. Because BSA-CuNCs or DPA-CuNCs in the mixture still maintains its intrinsic structure and performance, the use of double stabilizing agents is no benefit to improve the optical properties of CuNCs by the above scheme. To overcome the problem, we adopted another scheme, in which all Cu^{2+} in the system was reduced into Cu^{0} in the presence of DPA to form the DPA-CuNCs, and then introduced BSA to further form BSA/DPA-CuNCs (shown in Fig.1). The resulting CuNCs offer a similar fluoresence emission spectrum with sole DPA-CuNCs, verifying that the introduction of BSA does not lead to the formation of BSA-CuNCs and the damage of DPA-CuNCs. Owing to avoiding the reaction of BSA with Cu^{2+}, all BSA will be adsorbed on the surface of DPA-CuNCs to form an inert BSA shell on the DPA-CuNCs surface. In addition, the reaction conditions for synthesis of BSA/DPA-CuNCs were also optimized, including the reaction time for praparation of DPA-CuNCs and the

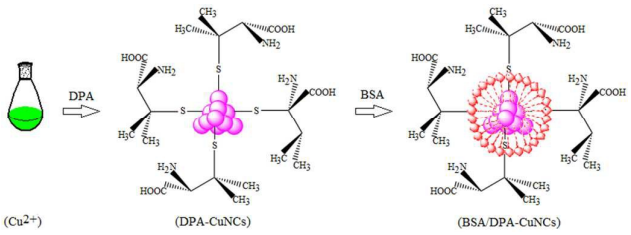

Fig.1 Procedure for the synthesis of BSA/DPA-CuNCs

amounts of BSA. Due to weak reduction ability of DPA, the formation of DPA-CuNCs requires a relatively long process. Fig.s2 shows that the synthesis of DPA-CuNCs needs a 90-minute reaction time at least. The resulted DPA-CuNCs gives the zeta potential of +35.2 mV, indicating a strong positive charge. In the study, the interaction of DPA-CuNCs with BSA was monitored by the zeta potential measurement. As BSA is negatively charged with electricity, their mixing will lead to rapidly produce BSA/DPA-CuNCs by their electrostatic attraction. Zeta potential of the DPA-CuNCs system immediately decreases with adding BSA (shown in Fig.s3), verifying the formation of BSA/DPA-CuNCs. The relationship of the peak fluorescence intensity with the amounts of BSA is presented in Fig.2. The peak fluorescence intensity will rapidly increase with the increase of the BSA concentration when the BSA conccentration is less than 0.01 mg ml^{-1}. Then, the peak fluoresence intensity reaches its maximum value. Continue to increase the concentration of BSA, the fluoresence intensity can remain almost unchanged. To obtain a high fluorescence emission, the BSA concentration of 0.02 mg ml^{-1} was employed for the synthesis.

To further understand the interaction of DPA-CuNCs with BSA, synchronous fluorescence and CD technologies were used to investigate the effect of DPA-CuNCs on the structure of BSA. As shown in Fig.s4, the synchronous fluorescence intensities of BSA obviously increase after added DPA-CuNCs for Δλ of both 15nm and 60 nm. Often, the Δλ of 15 nm or 60 nm may offer the characteristic information about the environmental changes of Tyr or Trp residues in BSA, respectively. Thus, the results demonstrates that the interaction of DPA-CuNCs with BSA changes the configuration of BSA, indicating an increased exposure of Tyr and Trp residues in the BSA. However, the results of CD analysis in Table s1 reveal that the change did not cause obvious damage of the secondary structures in BSA. Based on the above results, we suggest that the electrostatic attraction make DPA-CuNC and BSA close to each other and are accompanied by a small change in the configuration of BSA. Such a configuration change let DPA-CuNC enters into center of the BSA and finally form an inert BSA shell on the DPA-CuNC surface.

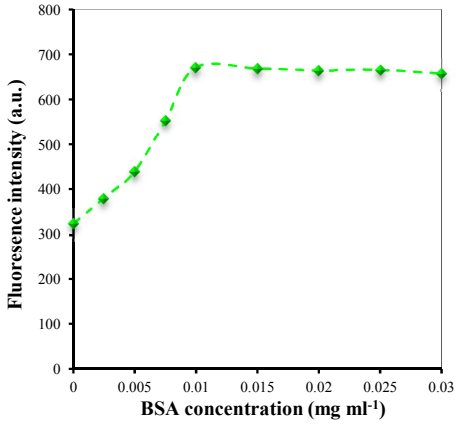

Fig.2 Effect of BSA concentration on the peak fluorescence intensity

3.2 Structure characterization

The as-prepared BSA/DPA-CuNCs product was characterized by TEM and XPS technologies. Bright field TEM image (Fig.3a) shows that most of the CuNCs exhibit approximately spherical shape with low degree of agglomeration. The Fig.3b presents the particle size distribution histogram, which is obtained using an image processing software. The size of the CuNCs is distributed in narrow range of 1-4 nm with the average particle size of ~2.2 nm. The standard deviation value (0.4nm) confirms the narrow size distribution of CuNCs.

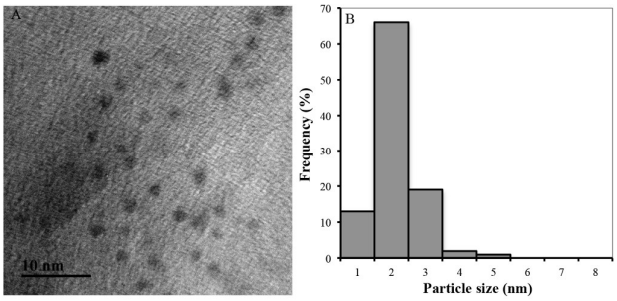

Fig.3 TEM (A) and particle size distribution histogram (B) of BSA/DPA-CuNCs

The XPS technology is powerful tool for studying on the surface chemical properties of materials. The C_{1s}, N_{1s}, S_{2p} and Cu_{2p} XPS spectra of BSA/DPA-CuNCs were shown in Fig.4. On the C_{1s} XPS spectrum there are five peaks. The peaks located at 284.4, 286.6 and 288.1eV can be assigned to C-C, C-O and C=O

species, respectively.[18] The XPS peak at 285 eV can be assigned to sp^2 C bonded to N. The peak at 288.8 eV can be assigned to O=C–O species. As binding energy of the element is related to its chemical environment in the material, the binding energy of the element moves to low energy position if the chemical environment of an element changes from a strong electron withdrawing environment to a relative low one. The peak at 287.7 eV can be assigned to the sp^3 C bonded to N, since the electronegative value of nitrogen is smaller than that of oxygen. On the N_{1s} XPS spectrum the peak at 398.4 eV can be assigned to N2, corresponds to pyridinic N. The peak at 399.8 eV can be assigned to amine. The peak at 401 eV can be assigned to N4 and corresponds to graphitic N. It was noteworthy that the peak intensity of amine nitrogen was remarkably bigger than that of pyridinic nitrogen and graphitic N, implying that amine nitrogen was dominant in the as-prepared CuNCs. This is because the DPA on the surface of BSA/DPA-CuNCs contains many amino groups. On the S_{2p} XPS spectrum there is a relatively strong peak at 165.7 eV, indicated the presence of chemisorbed S on the surface of CuNCs, which is supportive of the presence of Cu and S on the sample. On the Cu_{2p} spectrum there are two prominent peaks. The peaks at 952.1 and 932.7 eV could be assigned to $Cu_{2p1/2}$ and $Cu_{2p3/2}$, which were characteristic peaks due to Cu^0. The peak of Cu^+ can not distinguish from the peak of Cu^0, occurring at 0.1 eV apart from Cu^0.

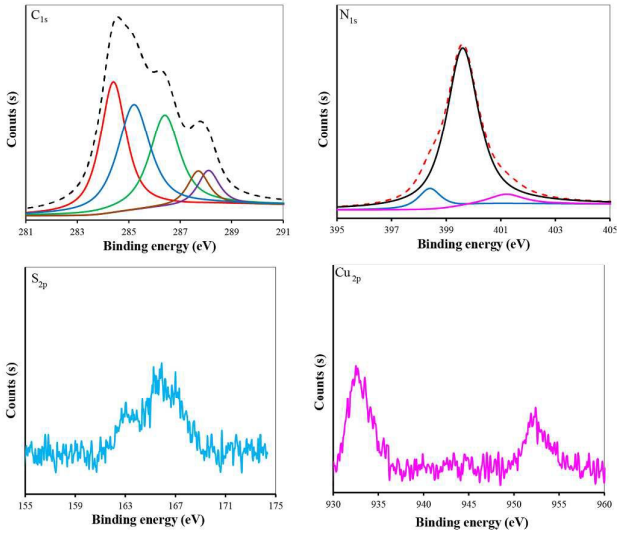

Fig.4 The C_{1s}, N_{1s}, S_{2p} and Cu_{2p} XPS spectra of BSA/DPA-CuNCs

3.3 The fluoresence intensity and photostability

The BSA/DPA-CuNCs as a novel optical probe offers a higher fluoresence intensity compared with DPA-CuNCs (shown in Fig.5). The intensity is more than 2-fold that of DPA-CuNCs, verifying that the introduction of BSA can remarkably enhance the fluorescence intensity. In addition, we also measured the quantum yields of CuNCs. The quantum yield of BSA/DPA-CuNCs is about 18.22%, which is higher than that of DPA-CuNCs (10.78%). The enhanced fluoresence intensity should be attributed to the electric neutralization and isolation effect of BSA. The DPA-CuNCs have strong positive charges, the withdrawing electron effect of these positive charges towards CuNCs will lead to an obvious decrease in the fluorescence intensity, leading to a weak fluorescence intensity. However, the addition of negatively charged BSA into the positively charged DPA-CuNCs reduces positive charge on the DPA-CuNC surface by electric neutralization. The action alleviates the withdrawing electron effect and enhances the fluorescence intensity. Thus, BSA/DPA-CuNCs shows a stronger fluorescence compared with DPA-CuNCs. Besides, the use of BSA also results in the formation of an inert BSA shell on the CuNCs surface. Such a BSA shell can effectively block the direct contact between the CuNC core and the water. This will greatly reduce the fluorescence quenching of water molecules towards CuNCs due to the solvent effect, further enhancing the fluorescence intensity.

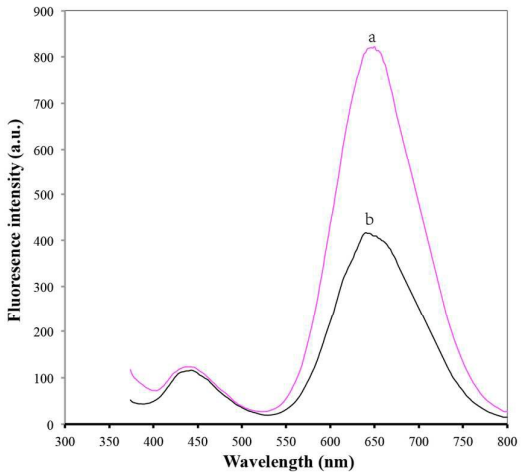

Fig.5 The fluorescence spectra of BSA/DPA-CuNCs (a) and DPA-CuNCs (b)

The photostability of BSA/DPA-CuNCs and DPA-CuNCs was investigated in the study. Here, a quartz cuvette filled with the CuNCs was placed under xenon lamp irradiation (300 W) and its fluorescence spectrum was measured on the fluorescence spectrophotometer. Fig.6 indicates that fluorescence intensity of the DPA-CuNCs slowly decreases with the increase of standing time, indicating a relatively poor photostability. This is because the part of DPA-CuNC surface is exposed to the outside. The characteristic make it is easy to be oxidized by oxygen in air, leading to a poor photostability. However, Fig.6b shows that the fluorescence intensity of BSA/DPA-CuNCs can keep almost unchanged within the irradiating time of 105 min, indicating an excellent photostability. Such an excellent photostability should be attributed to the protection of BSA shell on the CuNC surface.

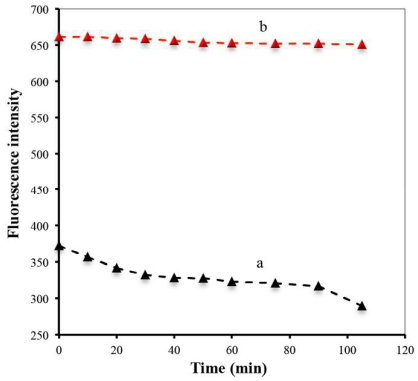

Fig.6 The peak fluorescence intensity of DPA-CuNCs (a) and BSA/DPA-CuNCs (b) with different standing time.

3.4 Fluorescence response towards Ag^+

Fluorecence response of the BSA/DPA-CuNCs towards Ag^+ was investigated in the laboratory. Fig.7 presents the fluorescence spectra of BSA/DPA-CuNCs in the presence and absence of 1.0×10^{-8} M Ag^+. It can be seen that the addition of Ag^+ brings an obvious fluorescence quenching. The peak fluorescence intensity change (ΔF) is up to 221 (about 36.8%). Based on the fluorescence quenching, the BSA/DPA-CuNC nanosensor was developed for the fluorescent detection of Ag^+. As a control sample, the DPA-CuNCs were also used for the fluorescence response test by using the same procedure. It was found that the addition of 1.0×10^{-8} M Ag^+ only cause a small fluorescence quenching (about 8.5%), verifying that the BSA/DPA-CuNCs have more sensitve reponse towards Ag^+ compared with DPA-CuNCs.

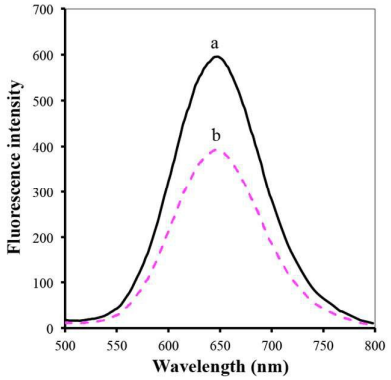

Fig.7 The fluorescence spectra of BSA/DPA-CuNCs in the presence and absence of 1.0×10^{-8} Ag^+ at pH 4.35.

The fluorescence quenching is generally classified as dynamic and static quenching. The former occurs due to collisional deexcitation of the fluorophore to the ground state while the latter takes place by forming non-fluorescent ground state complex between quencher and fluorophore. Dynamic and static quenching behaviors can be distinguished by investigating the fluorescence quenching rate constant at different temperatures. To study on the mechanism for the fluorescence response of BSA/DPA-CuNCs towards Ag^+, Stern–Volmer equation was used to investigate the fluorescence quenching data with respect to temperature:

$$\frac{F_0}{F} = 1 + K_{SV}C \qquad (1)$$

where F_0 and F denote steady-state fluorescence intensities in the absence and presence of Ag^+ respectively. K_{SV} is the Stern-Volmer quenching constant, and C is the concentration of Ag^+. According to Eqation (1), the slope of the F_0/F vs C yields the Stern–Volmer constant. The data points in the Stern–Volmer plot (shown in Fig.8), may be fitted linearly, which indicates that the quenching mechanism in the presence of Ag^+ is of the static type.[19]

The fluoresence quenching in the presence of Ag^+ should be attributed to the interaction of BSA/DPA-CuNCs with Ag^+, leading to form a non-fluorescent ground state complex. On the one hand, amino group in the DPA combines with Ag^+ to form stable coordination bond, leading to the fluorescence quenching. On the other hand, sulfydryl groups in the BSA combines with Ag^+ to form stable Ag-S covalent bond, further leading to the fluorescence quenching. More importantly, the special structure of BSA/DPA-CuNCs allows Ag^+ to simultaneity interact with amino group and sulfydryl group to form a stable complex. The action will result in a higher level of energy decrease compared with sole amino group or sulfydryl group.

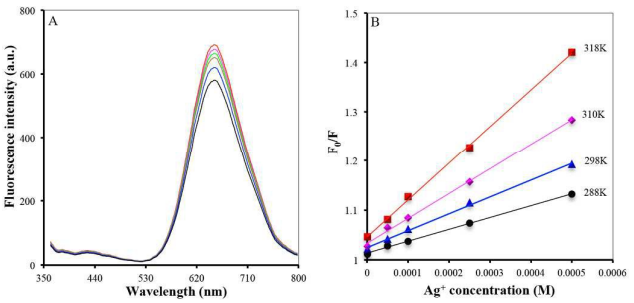

Fig.8A: The fluorescence spectra of BSA/DPA-CuNCs in the presence of 0.0, 0.000001, 0.00005, 0.0001, 0.00025 and 0.0005 M Ag^+ (from top to down). B: Stern-Volmer plot for the quenching of BSA/DPA-CuNCs by Ag^+ at five different temperatures.

3.5 Effects of the pH and ion strength

Effect of the pH in the medium on the detection of 1.0×10^{-8} Ag^+ using BSA/DPA-CuNCs as a nanosensor was investigate in the laboratory. Fig.9A shows the peak fluorescence retention rate (F/F_0) of BSA/DPA-CuNCs after added 1.0×10^{-8} Ag^+ in the BR of different pH without NaCl. Here, F and F_0 were the peak fluorescence intensity after and before added Ag^+, respectively. It can be seen that the F/F_0 can remain almost unchanged at pH between 1.5 and 5. When the pH exceed 5.0, the F/F_0 rapidly decreases with the increase of pH. When the pH is more than 7.0, the F/F_0 is close to zero. In order to understand the above effect, we measured the zeta potential and fluorescence intensity of BSA/DPA-CuNCs at different pH, respectively. It was found that the BSA/DPA-CuNCs have strong positive charge on the surface under the acid condition (pH<5). Due to strong electrostatic repulsion between the different CuNCs, the BSA/DPA-CuNCs exhibit an excellent

stability under the acid condition. More importantly, the repulsion greatly increases the distance between CuNCs. This behavior can effectively reduce the fluorescence quenching caused by the energy transfer between the CuNCs. However, positive charge of BSA/DPA-CuNCs will rapidly reduce with the increase of pH. The loss of surface charge tends to create serious CuNCs aggregation. The aggregation largely quickens the energy transfer between the CuNCs, thus resulting in the fluorescence quenching and insensitive response towards Ag^+. To obtain high sensitivity, the BR beffer of pH 4.35 was used in following experiments.

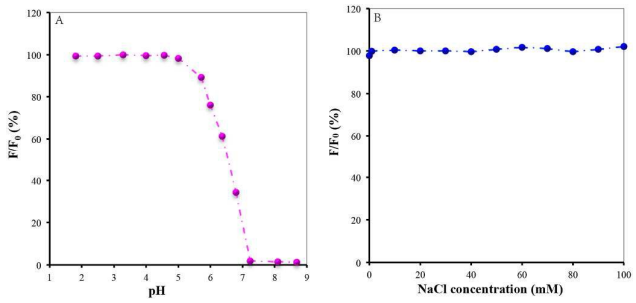

Fig.9 The peak fluorescence retention rate (F/F_0) of BSA/DPA-CuNCs after added 1.0×10^{-8} Ag^+ in the BR of different pH value without NaCl (A) and in the BR of pH 4.35 containing different concentration of NaCl (B)

Fig.9B presents the peak fluorescence retention rate (F/F_0) of BSA/DPA-CuNCs at the BR of pH4.35 containing different NaCl concentration after added 1.0×10^{-8} Ag^+. Here, F and F_0 were the peak fluorescence intensity after and before added Ag^+, respectively. Even in 1 M NaCl, only a 15% decrease of the F/F_0 was observed compared to that without NaCl, indicating that BSA/DPA-CuNCs could be applied in high ionic strength environments. The fluorescence intensity of CuNCs and the F/F_0 remained almost constant when exposed to 0.0-100 mM NaCl solutions, indicating the ionic strength had no significant effect on the fluorecent detection of Ag^+.

3.6 Analytical characteristics

The BSA/DPA-CuNCs were developed as new nanosensor for the fluorescent detection of Ag^+. Fig.10 shows fluorescence response of the nanosensor for different concentration of Ag^+ and the calibration plot of logarithmic Ag^+ content vs. corresponding peak fluorescence intensity. It can be seen that the fluorescence intensity decreases with the increase of Ag^+ concentration. The peak fluorescence intensity will linearly decrease with the increase of Ag^+ concentration in the range of 1.0×10^{-8}-1.0×10^{-16} M. The linear equation was $F=-18.583\times\log C +305.13$, with a statistically significant correlation coefficient of 0.9997, where F is the peak fluorescence intensity of BSA/DPA-CuNCs and C is Ag^+ concentration (M) in the solution. The detection limit was found to be 4.3×10^{-17} M that was obtained from the signal-to-noise characteristics of these data (S/N=3). The sensitivity is obviously higher than that of other optical methods in Table 1.

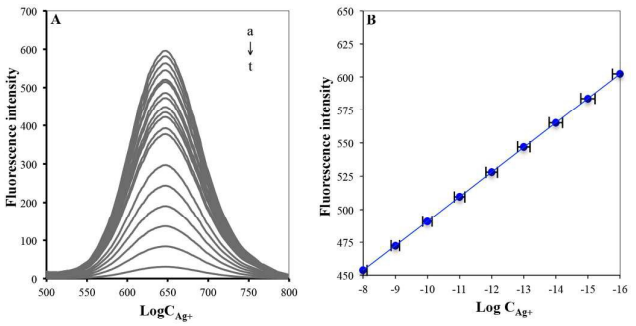

Fig.10A: Fluorescence spectra (A) of the BSA/DPA-CuNCs in 0.0, 1×10^{-16}, 1×10^{-15}, 1×10^{-14}, 1×10^{-13}, 1×10^{-12}, 1×10^{-11}, 5×10^{-10}, 1×10^{-9}, 5×10^{-8}, 5×10^{-7}, 1×10^{-6}, 1×10^{-5}, 1×10^{-4}, 1×10^{-3}, 1.6×10^{-3}, 2.5×10^{-3}, 4.0×10^{-3}, 6.0×10^{-3} and 1×10^{-2} M of Ag^{2+} (from a to t). B: The calibration plot of logarithmic Ag^+ concentration vs. fluorescence intensity at 642 nm.

The nanosensor was repeatedly measured for twenty times in 1.0×10^{-9} M of Ag^+ standard solution under the same conditions. The relative standard deviation of 2.9% for the measurements was obtained, indicating good precision. The BSA/DPA-CuNCs product was stored in at 4℃ and its sensitivity for the detection of 1.0×10^{-9} M Ag^+ was checked every week. The intensity can keep its initial response of 98.5% after the period of eighteen weeks, indicating an excellent long-term stability. The interference from possible cations and anions existed in environmental water for the detection of 1.0×10^{-9} M Ag^+ were investigated. K^+, Na^+, Ca^{2+}, Mg^{2+}, SO_4^{2-}, CO_3^{2-}, PO_4^{3-}, NO_3^- and Cl^- are main ions in environmental water. The result indicates that 50 mM of the each ion leads to far less than 5% of the fluorescence quenching. This is because the above ions do not react with the amino in the DPA and sulfydryl groups in the BSA attached on the surface of CuNCs. Cu^{2+}, Zn^{2+} and Ni^{2+} are at trace level in environmental water. These ions can combine with the amino and sulfydryl groups to form chemical bonds, which may lead to the fluorescence quenching. For example, the existence of 1.0 mM Cu^{2+} causes more than 42% of the fluorescence quenching. To eliminate their interferences, ethylene diamine tetraacetic acid (termed as EDTA) was added into the water sample prior to the BSA/DPA-CuNCs. Cu^{2+}, Zn^{2+} and Ni^{2+} can react with EDTA to form stable complexes, which cannot interact with the CuNCs and leads to the fluorescence quenching. The result shows that 0.5 mM of Cu^{2+}, Zn^{2+} or Ni^{2+} do not interfere with the fluorescent detection of Ag^+ when 1 mM of EDTA was used as masking agent.

Table 1 The comparison of methods for optical detection of silver ion

Material	Linear range (nM)	Limit of detection (nM)	Detection technique	Sample	Ref.
polyethylenimine - stabilized gold nanoparticles	1.09-1.09×10^2	1.09	colorimetric method	tap water drinking water	20
Thioflavin T/AgI supraparticle	1.0×10^2-1.0×10^4	50	fluorescent method	water	21
gold nanostar@Raman-reporter @silica sandwich structurture via DNA hybridization	0.001-10	1.7×10^{-3}	surface-enhanced Raman scattering	human saliva	22
E-3′,6′-dihydroxy-2-thiazol-2-ylmethylene)aminospiro [isoindoline-1,9′-xanthen]-3-one	1.0×10^2-1.0×10^4	80	fluorescent method	tap water, river water and lake water	23
photoluminescent polymer carbon nanoribbons	5-8.0×10^4	1.73	fluorescent method	Biological sample	24
BSA/DPA-CuNCs	1.0×10^{-1}-10	4.3×10^{-8}	fluorescent method	Natural water	Present work

3.7 Detection of silver ion in water samples

Feasibility of the proposed method for possible applications was investigated by analyzing water samples. In the study, tap water, ground water, lake water and river water samples used were collected from Jiangsu province in China. The recovery experiments were performed by measuring the fluorescence responses to the sample, in which the known concentrations of Ag^+ was added. The concentration of Ag^+ in water sample was determined from the calibration curve and the value was used to calculate the concentration in the original sample. The results of detection of Ag^+ in water samples are shown in Table 2. The recovery of Ag^+ in water samples ranged from 95.6 to 104.6%. These indicated proposed method has good accuracy and precision.

Table 2 The results of the detection of Ag^+ in water samples

Samples	Added (nM)	Found (nM)	Recovery (%)
Tap water	0.0	1.29	
	5.0	6.32	100.6
Ground water	0.0	4.16	
	5.0	9.10	98.8
Lake water	0.0	0.83	
	5.0	5.61	95.6
river water	0.0	1.02	
	5.0	6.25	104.6

4 Conclusions

The study demonstrated synthesis of D-penicillamine and bovine serum albumin co-stabilized copper nanoclusters. The as-prepared copper nanoclusters exhibit a better fluorescence intensity, photostability and response towards Ag^+ compared with D-penicillamine-stabilized copper nanoclusters. The copper nanoclusters have been used as novel nanosensor for fluorescent detection of Ag^+. The analytical method provides the advantage of sensitivity, repeatability and stability compared with present optical sensors for Ag^+. The study also opens a new avenue for fabrication of functional metal nanoclusters that hold great promise in the potential applications such as nanosensors, biocatalyst and molecular carriers.

Acknowledgements

The authors acknowledge financial supports from Colleges and Universities Graduate Research Innovation Project of Jiangsu province (KYLX15_1159), Prospective Joint Research Project: Cooperative Innovation Fund (BY2014023-01), National Natural Science Foundation of China (21176101), Fundamental Research Funds for Central Universities (JUSRP51314B) and MOE & SAFEA for the 111 Project (B13025).

Notes and references

[a] *School of Chemical and Material Engineering, Jiangnan University, Wuxi 214122, China. Fax:86051085811863; Tel:13912371144; e-mail: zaijunli@263.net; zaijunli@jiangnan.edu.cn.*

[b] *School of Food Science and Technology, Jiangnan University, Wuxi 214122, China*

[c] *Key Laboratory of Food Colloids and Biotechnology, Ministry of Education, Wuxi 214122, China*

† Electronic Supplementary Information (ESI) available: [details of any supplementary information available should be included here]. See DOI: 10.1039/b000000x/

1 K. Schouteden, K. Lauwaet, E. Janssens, G. Barcaro, A. Fortunellic, C.V. Haesendonck and P. Lievens, *Nanoscale*, 2014,**6**, 2170-2176.
2 B. Khlebtsov, E. Tuchina, V. Tuchinbcd and N. Khlebtsov, *RSC Adv*., 2015,**5**, 61639-61649.
3 L. Gong, H.L. Kuai, S.L. Ren, X.H. Zhao, S.Y. Huan, X.B. Zhang and W.H. Tan, *Chem. Commun*., 2015,**51**, 12095-12098
4 S. Meerod, B. Rutnakornpitud, U. Wichai and M. Rutnakornpituk, *J. Magn. Magn. Mater.*, 2015, **392**, 83-90; X.Y. Zhou, R.Y. Li, X.F. Wu and Z.J. Li, *Anal. Methods*, 2014, **6**, 2862-2869; X.Q. Liao, R.Y. Li, X.H. Long and Z.J. Li, *RSC Adv*., 2015, **5**, 48835-48841.
5 X.F. Wu, R.Y. Li and Z.J. Li, *RSC Adv*., 2014, **4**, 9935-9941.
6 X.Q. Liao, R.Y. Li, Z.J. Li, X.L. Sun, Z.P. Wang and J.K. Liu, *New J. Chem*., 2015, **39**, 5240-5248.
7 B. Pergolese, M. Muniz-Miranda and A. Bigotto, *J. Phys. Chem. B*, 2006, **110**, 9241-9245.
8 C.X. Wang, H. Cheng, Y.J. Huang, Z.Z. Xu, H.H. Lin and C. Zhang, *Analyst*, 2015, **140**, 5634-5639.
9 X.F. Wu, R.Y. Li, Z.J. Li, J.K. Liu, G.L. Wang and Z.G. Gu, *RSC Adv*., 2014, **4**, 24978-24985.
10 C.Y. Ke, Y.T. Wu, W.L. Tseng, *Biosens. Bioelectron*., 2015, **69**, 46-53.
11 T. Zhao, X.W. He, W.Y. Li and Y.K. Zhang, *J. Mater. Chem. B*, 2015,**3**, 2388-2394.
12 C.J. Yu, T.H. Chen, J.Y. Jiang and W.L. Tseng, *Nanoscale*, 2014, **6**, 9618-9624.
13 H. Huang, H. Li, A.J. Wang, S.X. Zhong, K.M. Fang and J.J. Feng, *Analyst*, 2014, **139**, 6536-6541.
14 Z.Y. Wang, L. Si, J.C. Bao and Z.H. Dai, *Chem. Commun.*, 2015,**51**, 6305-6307.
15 D.Q. Feng, G.L. Liu and W. Wang, *J. Mater. Chem. B*, 2015, **3**, 2083-2088.
16 X.M. Yang, Y.J. Feng, S.S. Zhu, Y.W. Luo, Y.Zhuo and Y. Dou, *Anal. Chim. Acta*, 2014, **847**, 49-54.
17 R. Ghosh, A. K. Sahoo, S.S. Ghosh, A. Paul and R. Chattopadhyay, *ACS Appl. Mater. Interfaces*, 2014, **6**, 3822-3828.
18 Z.G. Mou, X.Y. Chen, Y.K. Du, X.M. Wang, P. Yang, S.D. Wang, *Appl. Surf. Sci.*, 2011, **258**, 1704.
19 M.R. Eftink, C.A. Ghiron, Anal. Biochem., 1981, **114**,199-202.
20 Y. Liu, Y. Liu, Z.F. Li, J.S. Liu, L. Xu and X.Y. Liu, *Analyst*, 2015, **140**, 5335-5343.
21 Y.Y. Li, M. Zhang, L.F. Lu, A.W. Zhu, F. Xia, T.S. Zhou and G.Y. Shi, *Analyst*, 2015, DOI: 10.1039/C5AN01146A.
22 P. Zheng, M. Li, R. Jurevic, S.K. Cushing, Y.X. Liu and N.Q. Wu, *Nanoscale*, 2015, **7**, 11005-11012.
23 D.S. Lin, J.P. Lai, H. Sun, Z. Yang and Y. Zuo, *Anal. Methods*, 2014, **6**, 1517-1522.
24 Z.X. Wang and S.N. Ding, *Anal. Chem.*, 2014, **86**, 7436-7445.

D-penicillamine and bovine serum albumin co-stabilized copper nanoclusters with remarkably enhanced fluorescence intensity and photostability for ultrasensitive detection of Ag^{+}

Li Ruiyi,[a] Wang Huiying,[a] Zhou Xiaoyan,[a] Liao Xiaoqing,[a] Sun Xiulan[b] and Li Zaijun*[a,c]

[a] *School of Chemical and Material Engineering, Jiangnan University, Wuxi 214122, China*

[b] *School of Food Science and Technology, Jiangnan University, Wuxi 214122, China*

[c] *Key Laboratory of Food Colloids and Biotechnology, Ministry of Education, Wuxi 214122, China*

The study reported synthesis of D-penicillamine and bovine serum albumin co-stabilized copper nanoclusters (BSA/DPA-CuNCs). The BSA/DPA-CuNCs exhibit a better fluorescence intensity, stability and response towards silver ion compared with DPA-CuNCs. The nanosensor based on the BSA/DPA-CuNCs has been successfully used for the detection of Ag^{+} in water.